Andrographis exerts antitumor effects and enhances 5-FU efficacy via the alteration of ferroptosis-related genes in esophageal squamous cell carcinoma

KOSUKE YOSHIMURA[1,2*], TADANOBU SHIMURA[1*], RUIYA MA[1*], YAXUAN HUANG[1], TAKAHITO KITAJIMA[1,3], SHINJI YAMASHITA[1], YUKI SATO[1], KOKI HIGASHI[1], MIKIO KAWAMURA[1], HIROMI YASUDA[1], YUHKI KOIKE[1], YOSHIKI OKITA[1], SHIGEYUKI YOSHIYAMA[1], MINAKO KOBAYASHI[1,4], MASAKI OHI[1], HIROKI OHGE[2], SHINYA TAKAHASHI[2], AJAY GOEL[5], YOSHINAGA OKUGAWA[1,3] and YUJI TOIYAMA[1]

[1]Department of Gastrointestinal and Pediatric Surgery, Institute of Life Sciences, Mie University Graduate School of Medicine, Tsu, Mie 514-8507, Japan; [2]Department of Surgery, Graduate School of Biomedical and Health Sciences, Hiroshima University, Hiroshima 734-8551, Japan; [3]Department of Genomic Medicine, Mie University Hospital, Mie 514-8507, Japan; [4]Division of Reparative Medicine, Institute of Life Sciences, Mie University Graduate School of Medicine, Mie 514-8507, Japan; [5]Department of Molecular Diagnostics and Experimental Therapeutics, Beckman Research Institute, City of Hope Comprehensive Cancer Center, Duarte, CA 91016, USA

Received September 28, 2025; Accepted March 4, 2026

DOI: 10.3892/or.2026.9104

Abstract. Preoperative systemic chemotherapy plays a crucial role in enhancing the outcomes of patients with locally advanced esophageal squamous cell carcinoma (ESCC). Andrographis (major bioactive diterpenoid lactone isolated from *Andrographis paniculata*; PubChem ID: 5318517), a safe and cost-effective dietary compound, has demonstrated antitumor effects against various gastrointestinal adenocarcinomas. However, its impact on squamous cell carcinoma remains unclear. The present study explored the antitumor effects of Andrographis and its potential to augment the antitumor efficacy of 5-fluorouracil (5-FU). A series of *in vitro* experiments was conducted, including cell proliferation, colony formation and apoptosis assays, using the ESCC cell lines KYSE410 and TE1. Compared with the controls, Andrographis significantly inhibited cell proliferation (P<0.05), suppressed colony formation (P<0.05), induced apoptosis (P<0.05), and upregulated the expression of ferroptosis-related genes and proteins, such as HMOX1 (P<0.01), GCLC (P<0.05) and GCLM (P<0.001). Notably, even at a sub-IC_{50} dose of 5-FU, its combination with Andrographis resulted in additive antitumor effects (P<0.05) and further upregulation of ferroptosis-related gene expression, particularly HMOX1 (P<0.05), compared with either mono-treatment. The findings of the present study indicate that Andrographis exerts antitumor effects and enhances the efficacy of 5-FU in ESCC by activating both apoptosis and ferroptosis, suggesting its potential as an adjunctive therapy for ESCC to improve efficacy and reduce 5-FU dosage and toxicity.

Correspondence to: Dr Tadanobu Shimura, Department of Gastrointestinal and Pediatric Surgery, Institute of Life Sciences, Mie University Graduate School of Medicine, 2-174 Edobashi, Tsu, Mie 514-8507, Japan
E-mail: tadanobu189222@gmail.com

*Contributed equally

Abbreviations: 5-FU, 5-fluorouracil; C.I., combination index; ESCC, esophageal squamous cell carcinoma; FBS, fetal bovine serum; HMOX1, heme oxygenase-1; GAPDH, glyceraldehyde 3-phosphate dehydrogenase; GCLC, glutamate-cysteine ligase catalytic; GCLM, glutamate-cysteine ligase modifier; GPX4, glutathione peroxidase 4; GSH, glutathione; MSS, microsatellite stable; ROS, reactive oxygen species

Key words: andrographis, 5-FU, ESCC, antitumor effect, chemosensitization, ferroptosis

Introduction

Esophageal cancer (EC) is the seventh leading cause of cancer-related deaths worldwide and is mainly classified as esophageal squamous cell carcinoma (ESCC) and adenocarcinoma (1). Advances in endoscopic techniques have improved the accuracy of tumor staging; however, even when tumors are confined to the mucosa, lymph node metastasis occurs in 10-15% of patients with tumor invasion of the muscularis mucosae (2). Consequently, EC is associated with a poor prognosis, with a 5-year survival rate <20% (2). Despite advances in therapy, patient outcomes remain unsatisfactory, and EC continues to pose a significant challenge to global health. This highlights the need for improved diagnostic methods and treatment strategies for EC.

EC treatment primarily involves surgery, including endoscopic or surgical resection, often combined with chemotherapy. For ESCC, the Japan Clinical Oncology Group (JCOG) trials have shown improved overall survival (OS) with

neoadjuvant chemotherapy (NAC) using cisplatin and 5-fluorouracil (5-FU) (CF) in locally advanced ESCC (JCOG9907) (3) and further OS benefit when docetaxel is added to CF (DCF) (JCOG1109) (4). However, key agents such as 5-FU can cause severe toxicities, and prolonged 5-FU administration can promote resistance through complex, multifactorial mechanisms involving altered DNA damage responses and signaling pathway activities (5-7), resulting in reduced efficacy against ESCC. Moreover, the high cost of treatment further complicates the balance between efficacy, safety and cost.

Given their low toxicity and cost-effectiveness, complementary and alternative medicines, especially dietary compounds, have emerged as compelling areas of study. Andrographis, a C20-diterpenoid lactone derived from *Andrographis paniculata* and a component of traditional Indian medicine, has been used historically to treat fever, infections and gastrointestinal disorders (8-10). Because Andrographis is structurally stable in circulation (11-13), it exhibits anti-inflammatory, immunomodulatory and antitumor activities. Its antitumor effects have been demonstrated in gastric, colorectal and pancreatic adenocarcinomas, suggesting broad efficacy across gastrointestinal cancers (14-18). Importantly, the authors' previous study focused on ferroptosis. Ferroptosis, an iron-dependent, lipid peroxidation-driven regulated cell death pathway (19-21), has emerged as a potential mechanism, suggesting that Andrographis may exert antitumor effects through ferroptosis in adenocarcinomas. However, evidence in squamous cell carcinomas (SCCs) is scarce (22,23), and whether Andrographis activates ferroptosis in ESCC remains unclear.

Although the anticancer effects of andrographolide in ESCC have been described previously, the potential modulation of ferroptosis-related transcriptional programs in ESCC, particularly under combination treatment with 5-FU, has not been investigated. Therefore, the present study aimed to evaluate the antitumor effect of Andrographis in ESCC and to determine whether combination treatment with 5-FU modulates ferroptosis-associated gene expression and redox-related pathways.

Materials and methods

Cell culture and materials. The EC cell lines KYSE410 [poorly differentiated SCC, Microsatellite Stable (MSS) and TE1 (well-differentiated SCC, MSS)] were supplied by the Cell Resource Center of Biomedical Research, Institute of Development, Aging, and Cancer (Tohoku University). The identity of the cell line was confirmed by assessing the genetic and epigenetic markers. The cultures were periodically tested for mycoplasma contamination. Cells were cultured in Roswell Park Memorial Institute (RPMI)-1640 medium (Nacalai Tesque, Inc.) enriched with 10% fetal bovine serum (FBS; Biowest) and an antibiotic-antimycotic cocktail (Nacalai Tesque, Inc.). The cells were incubated at 37˚C in a humidified incubator with 5% CO_2. Andrographis was kindly provided by Professor Ajay Goel (City of Hope Comprehensive Cancer Center). The compound was manufactured by EuroPharma USA. According to the manufacturer's certificate of analysis, the preparation is a purified extract of *Andrographis paniculata* and contains 80% Andrographolide as the principal active constituent. Chemical characterization, including the standardization of Andrographolide content and purity confirmation, was based on the manufacturer's certificate of analysis. No additional extraction or purification was performed outside EuroPharma USA for the present study. For all assays, the compound was dissolved in DMSO to prepare a stock solution, which was subsequently diluted with the culture medium to the indicated final concentrations.

Cell viability and proliferation assay. For Water Soluble Tetrazolium (WST) assay, 4,000 cells/well were seeded in 96-well tissue culture plates (TPP Techno Plastic Products AG). The cells were cultured in RPMI-1640 medium supplemented with 10% FBS and antibiotics and allowed to adhere overnight. Subsequently, ESCC cells were exposed to various concentrations of 5-FU and Andrographis for 72 h. The tested doses were 3, 3.5, 4, 4.5 and 5 μM for 5-FU, and 36, 42, 48, 54 and 60 μg/ml for Andrographis, respectively. This procedure was performed to determine the cytotoxic effects of these compounds. Cell proliferation was measured using WST 8 (Dojindo Laboratories, Inc.) according to the manufacturer's instructions. Based on the inhibitory concentration at 50% (IC_{50}) (24), a combination of 5-FU and Andrographis (3, 3.5, 4, 4.5 and 5 μM and 36, 42, 48, 54, and 60 μg/ml) was used to treat each cell line for 72 h. Absorbance values were measured for each well at a wavelength of 450 nm using SoftMax Pro microplate reader (Molecular Devices, LLC.). To maintain consistency across the experimental conditions, an identical final concentration of DMSO was applied to all treatment groups, including the control group. The interaction between 5-FU and Andrographis was quantitatively assessed by calculating the combination index (C.I.) at the IC_{50} using the Chou-Talalay method (24). C.I. values were generated using GraphPad Prism ver. 10.0 (GraphPad Software Inc.; Dotmatics) and a C.I. <1.0 was regarded as suggestive of additive effects (24). Each experiment was independently repeated three times, with technical triplicates included in each of the biological replicates.

Cell colony formation assay. Colony formation assays were performed based on established protocols (25) with minor procedural adaptations. Specifically, KYSE410 and TE1 cells were seeded in 6-well tissue culture plates (TPP Techno Plastic Products AG) at a density of 500 cells/well, using an identical culture medium. The plates were incubated for 24 h. A total of 1 ml/well of 5-FU (3.5 μM), Andrographis (42 μg/ml), and a combination of 5-FU and Andrographis (3.5 μM, 42 μg/ml) were then added for 72 h. Following the initial incubation, the medium was replaced with fresh drug-free culture medium. The cells were then cultured at 37˚C with 5% CO_2 in a humidified environment for 7-9 days. Colonies consisting of at least 50 cells were counted as a colony. Colony numbers were quantified using ImageJ software ver.1.54p (National Institutes of Health) (26). These counts were then compared between the control and drug treatment groups.

Cell apoptosis assay. Apoptosis was assessed using propidium iodide/annexin V double staining and flow cytometry. Cells were inoculated into a 6-well tissue culture plate at a density of $1.6x10^5$ cells/well and pre-incubated for 24 h. Subsequently, the cultures were treated with one of the following treatments

for 72 h: 5-FU (3.5 μM), Andrographis (42 μg/ml), or a combination of 5-FU and Andrographis (3.5 μM, 42 μg/ml) for 72 h. Apoptotic cells were measured using Muse® Annexin V and Dead Cell Assay (Luminex Corporation) on a Muse™ Cell Analyzer (Merck KGaA), following the manufacturer's instructions. Data acquisition and analysis were performed using Muse Cell Analyzer software (version 1.4; Merck KGaA).

Quantitative mRNA expression analysis. To quantify mRNA expression, cells were seeded in 6-well tissue culture plates at a density of $3.0x10^5$ cells/well. After a 24 h adherence period, the cultures were subjected to drug treatment. Specifically, the cells were exposed to 5-FU (3.5 μM), Andrographis (42 μg/ml), or a combination of 5-FU and Andrographis (3.5 μM, 42 μg/ml). Total RNA was extracted from the cells using an RNA extraction miRNeasy Mini kit (Qiagen GmbH). Complementary DNA (cDNA) was synthesized from 5.0 ng of total RNA using a Reverse Transcription kit (Toyobo Co., Ltd.) according to the manufacturer's instructions. Reverse transcription-quantitative polymerase chain reaction (RT-qPCR) was performed using cDNA and the Power SYBR® Green PCR Master Mix (Thermo Fisher Scientific Inc.). RT-qPCR analysis was conducted using a StepOne™ Real-Time PCR System (Thermo Fisher Scientific, Inc.). The thermocycling conditions were as follows: Initial denaturation at 95˚C for 10 min, followed by 40 cycles of denaturation at 95˚C for 15 sec and annealing/extension at 60˚C for 60 sec. The primer sequences were as follows: heme oxygenase 1 (HMOX1) forward, 5'-AAGACTGCGTTCCTGCTCAAC-3' and reverse, 5'-AAAGCCCTACAGCAACTGTCG-3'; glutamate cysteine ligase catalytic (GCLC) forward, 5'-AGGCCAACATGC GAAAAC-3' and reverse, 5'-CGGATATTTCTTGTTAAG GTACTGG-3'; glutamate cysteine ligase modifier (GCLM) forward, 5'-TTGGAGTTGCACAGCTGGAT-3' and reverse, 5'-GGTTTTACCTGTGCCCACTGA-3'; glutathione peroxidase 4 (GPX4) forward, 5'-GAGGCAAGACCGAAGTAAACT AC-3' and reverse, 5'-CCGAACTGGTTACACGGGAA-3'; solute carrier family 7 member 11 (SLC7A11) forward, 5'-TCT CCAAAGGAGGTTACCTGC-3' and reverse, 5'-AGACTC CCCTCAGTAAAGTGAC-3'; nuclear factor kappa B subunit 1 (NFKB1) forward, 5'-AACAGAGAGGATTTCGTTTCC G-3' and reverse, 5'-TTTGACCTGAGGGTAAGACTTCT-3'; signal transducer and activator of transcription 3 (STAT3) forward, 5'-ACCAGCAGTATAGCCGCTTC-3' and reverse, 5'-GCCACAATCCGGGCAATCT-3'; NFE2 like bZIP transcription factor 2 (NFE2L2) forward, 5'-TCCAGTCAGAAA CCAGTGGAT-3' and reverse, 5'-GAATGTCTGCGCCAA AAGCTG-3'; acyl-CoA synthetase long chain family member 4 (ACSL4) forward, 5'-AACCCAGAAAACTTGGGCATT-3' and reverse, 5'-GTCGGCCAGTAGAACCACT-3'; and glyceraldehyde 3-phosphate dehydrogenase (GAPDH) forward, 5'-GGAAGGTGAAGGTCGGAGTC-3' and reverse, 5'-AAT GAAGGGGTCATTGATGG-3'. Target gene expression levels were quantified using the $2^{-\Delta\Delta Cq}$ method (27). The resulting values were subsequently standardized to the housekeeping gene, GAPDH.

Western blotting. ESCC cells ($7.5x10^5$ cells/well) were treated with 5-FU (3.5 μM), Andrographis (42 μg/ml), and a combination of 5-FU and Andrographis (3.5 μM, 42 μg/ml) for 72 h. The control group received RPMI-1640 medium enriched with 10% FBS and an antibiotic-antimycotic cocktail. Cells were lysed in Radioimmunoprecipitation Assay buffer (BioDynamics Laboratory, Inc.) supplemented with a proteinase inhibitor cocktail (Sigma Aldrich; Merck KGaA). Protein quantification was performed using a BCA Protein Assay Kit (Thermo Fisher Scientific, Inc.). Subsequently, the samples were combined with the loading buffer and denatured by boiling for 5 min. Equal amounts of protein (20 μg per lane) were loaded. The samples were subjected to electrophoresis on 4-15% gradient Mini-PROTEAN®TGX™ (Bio-Rad Laboratories, Inc.) for 50 min and transferred to PVDF membranes using Trans-Blot®Turbo™ (Bio-Rad Laboratories, Inc.) with EB RAPID for 5 min. The membranes were initially incubated with 5% milk for 60 min at room temperature for blocking purposes. The membranes were then exposed to the indicated primary antibodies for 60 min at room temperature. mouse monoclonal anti HMOX1 (1:1,000; cat. no. sc-136960), mouse monoclonal anti-γ-GCLC (1:2,000; cat. no. sc-390811) and mouse monoclonal anti-γ-GCLM (1:5,000; cat. no. sc-55586; all from Santa Cruz Biotechnology, Inc.). The membranes were then washed three times with Tris buffer saline containing 0.05% Tween 20 at room temperature. Following washing, the membranes were probed with anti-mouse IgG (cat. no. W4028; Promega Corporation) as the secondary antibody for 30 min at room temperature. The secondary antibody was applied at the following dilutions: 1:10,000 for HMOX1, and 1:20,000 for γ-GCLC, and 1:20,000 for γ-GCLM. Mouse monoclonal β-actin antibody (691001; MP Biomedicals, LLC) was used as the loading control. Protein signals were visualized using a chemiluminescent imaging system (ATTO Corporation) after incubation with Immobilon® Western (MilliporeSigma).

Statistical analysis. Statistical analyses were performed for each experiment as follows: Cell viability and proliferation assay: For comparisons across multiple treatment groups, one-way ANOVA followed by Tukey's post hoc test was performed. Differences among multiple treatment conditions were analyzed using one-way ANOVA with Tukey's post hoc test regarding ell colony formation assays. Percentages of apoptotic cells in cell apoptosis assay were compared using one-way ANOVA followed by Tukey's post hoc test. Relative mRNA expression levels were compared using one-way ANOVA with Tukey's post hoc test. Data are presented as the mean ± standard error of the mean (SEM). Statistically significant difference was defined as $P<0.05$. Analyses were conducted using JMP® Pro ver. 18.0.2 (SAS Institute Inc.) and GraphPad Prism ver. 10.5.0 (Dotmatics).

Results

Andrographis demonstrates anti-proliferative effects and synergizes with 5-FU in ESCC cells. To assess whether Andrographis has proliferation-inhibitory effects on ESCC cells and whether it additively enhances the cell proliferation inhibitory effect of 5-FU on ESCC cells, KYSE410 and TE1 were used to examine the effects of 5-FU (3, 3.5, 4, 4.5 and 5 μM) and Andrographis (36, 42, 48, 54 and 60 μg/ml) individually and in combination on cell proliferation. WST assay results indicated that Andrographis exhibited significantly greater proliferation

inhibitory activity than 5-FU in both cell lines (P<0.05). Moreover, the combination of 5-FU and Andrographis significantly inhibited cell proliferation compared with individual treatments in both cell lines (P<0.05) (Fig. 1A).

Notably, both 5-FU and Andrographis inhibited the proliferation of KYSE410 and TE1 cells in a dose-dependent manner, with IC_{50} values of 14.0 and 4.5 μM for 5-FU and 51.7 and 40.9 μg/ml for Andrographis, respectively. Moreover, when used in combination, the IC_{50} value was further reduced, and the evaluation of the C.I. demonstrated an additive effect between 5-FU and Andrographis in both cell lines (Fig. 1B). These findings suggest that Andrographis inhibits ESCC cell proliferation, and the combination with 5-FU may enhance this inhibitory effect, following the defined criteria (28). Based on these findings, to avoid excessive cytotoxicity caused by 5-FU while enabling evaluation of whether Andrographis has an additive effect, subsequent assays were conducted using a sub-IC_{50} concentration of 5-FU (3.5 μM).

Andrographis serves as a sensitizer or adjunct to 5-FU in suppressing colony formation in ESCC cells. Next, the effects of 5-FU, Andrographis, and their combination on cell viability were investigated using colony formation assays. In KYSE410 cells, both 5-FU and Andrographis significantly reduced colony formation compared with the control (P<0.001) (Fig. 2A). In TE1 cells, 5-FU did not significantly alter colony formation, whereas Andrographis significantly decreased the colony number (P<0.05) (Fig. 2B). In both cell lines, combination treatment showed a greater reduction in colony numbers than 5-FU alone. However, the extent of reduction was comparable to that observed with Andrographis alone, and no significant difference was detected between the two groups. Thus, while the combination treatment did not show a clear additional reduction compared with treatment with Andrographis alone, it exhibited a more noticeable inhibitory effect relative to 5-FU alone.

Andrographis treatment potentiates the effects of 5-FU through increased apoptosis in ESCC cells. Previous studies have indicated that Andrographis induces apoptosis in various gastrointestinal adenocarcinoma cells (14-18). Next, it was assessed whether the observed suppression of cell viability following treatment with 5-FU, Andrographis, and the combination was correlated with an increase in apoptosis in ESCC cells. An Annexin V binding assay was performed to quantify apoptotic cells after individual and combination treatments. As shown in Fig. 3, Andrographis significantly elevated the apoptotic rate compared with the control, particularly in TE1 cells (P<0.05). Furthermore, the combination treatment led to a further increase in the percentage of apoptotic cells compared with the control: 20.8% vs. 14.9% in KYSE410 cells (P<0.001) (Fig. 3A) and 48.5% vs. 11.7% in TE1 cells (P<0.0001) (Fig. 3B). Consistent with the enhanced suppression of cell viability observed with combination treatment, a significantly higher percentage of apoptotic cells was observed compared with that observed with individual treatments (P<0.05) (Fig. 3A and B). These findings suggest that Andrographis not only induces apoptosis in ESCC cells but also enhances 5-FU-mediated apoptosis, potentially acting as a sensitizer or adjunct agent for chemotherapy.

Andrographis exerts its antitumor effect via upregulation of ferroptosis-associated genes. Previously, it was reported that Andrographis upregulates ferroptosis-related genes, such as HMOX1, GCLC and GCLM, in gastric and colorectal adenocarcinoma cells (14,16,17). Other studies have shown that Andrographis activates ferroptosis in several malignant tumors, such as non-small cell lung cancer (29) and multiple myeloma (30) cells. To determine whether this finding is applicable to ESCC cells, RT-qPCR and western blotting assays were performed, focusing on HMOX1, GCLC and GCLM as the key target genes in ferroptosis.

As shown in Fig. 4A, HMOX1 (KYSE410 P<0.01; TE1 P<0.01), GCLC (KYSE410 P<0.001; TE1 P<0.05) and GCLM (KYSE410 P<0.001; TE1 P<0.0001) were significantly upregulated in ESCC cells after treatment with Andrographis compared with the control. Combination treatment also upregulated HMOX1 (KYSE410 P<0.0001; TE1 P<0.01), GCLC (KYSE410 P<0.001; TE1 P<0.05) and GCLM (KYSE410 P<0.001; TE1 P<0.001) at the mRNA level compared with the control. Furthermore, HMOX1 (KYSE410 P<0.0001; TE1 P<0.001), GCLC (KYSE410 P<0.001; TE1 P<0.01) and GCLM (KYSE410 P<0.001; TE1 P<0.001) were significantly upregulated by the combination treatment compared with those treated with 5-FU in both ESCC cell lines.

Western blotting was performed to validate the expression of HMOX1, GCLC and GCLM at the protein level. As shown in Fig. 4B, the expression levels of HMOX1, GCLC and GCLM at the protein level were increased in both the Andrographis and combination treatment groups compared with those in the control and 5-FU groups in both ESCC cell lines.

Regarding mRNA expressional alteration of other ferroptosis related genes such as NF-kB (NFKB1), STAT3, Nrf2 (NFE2L2) and ACSL4, these targets did not show consistent trends between untreated/individual/combination treatment groups in two ESCC cell-lines (Fig. S1). In case of GPX4, mRNA expression of GPX4 was downregulated and showed similar trends after Andrographis or combination treatment in two ESCC cell-lines (Fig. S1). On the other hand, mRNA expression of SLC7A11 were upregulated and showed similar trends after Andrographis or combination treatment (Fig. S1).

Discussion

In the present study, the antitumor effects of Andrographis against ESCC cells (KYSE410 and TE1) were examined and its additive effects with 5-FU, a key agent of systemic chemotherapy for ESCC, were evaluated. It was demonstrated that Andrographis inhibited cell proliferation and colony formation and induced cell death through the activation of apoptosis and ferroptosis. Using a sub-IC_{50} dose of 5-FU minimized cytotoxicity and enabled proper evaluation of its single-agent effects. Even at this low dose, combining 5-FU with Andrographis further enhanced the response. These findings align with prior reports of Andrographis activity in ESCC and suggest its potential as a 5-FU-based adjunct therapy.

The standard treatment for locally advanced EC is NAC followed by curative surgery. The JCOG9907 and JCOG1109 trials demonstrated the efficacy of CF and DCF therapies, respectively, as promising NAC regimens (3,4). However, both regimens frequently cause severe toxicities, including febrile

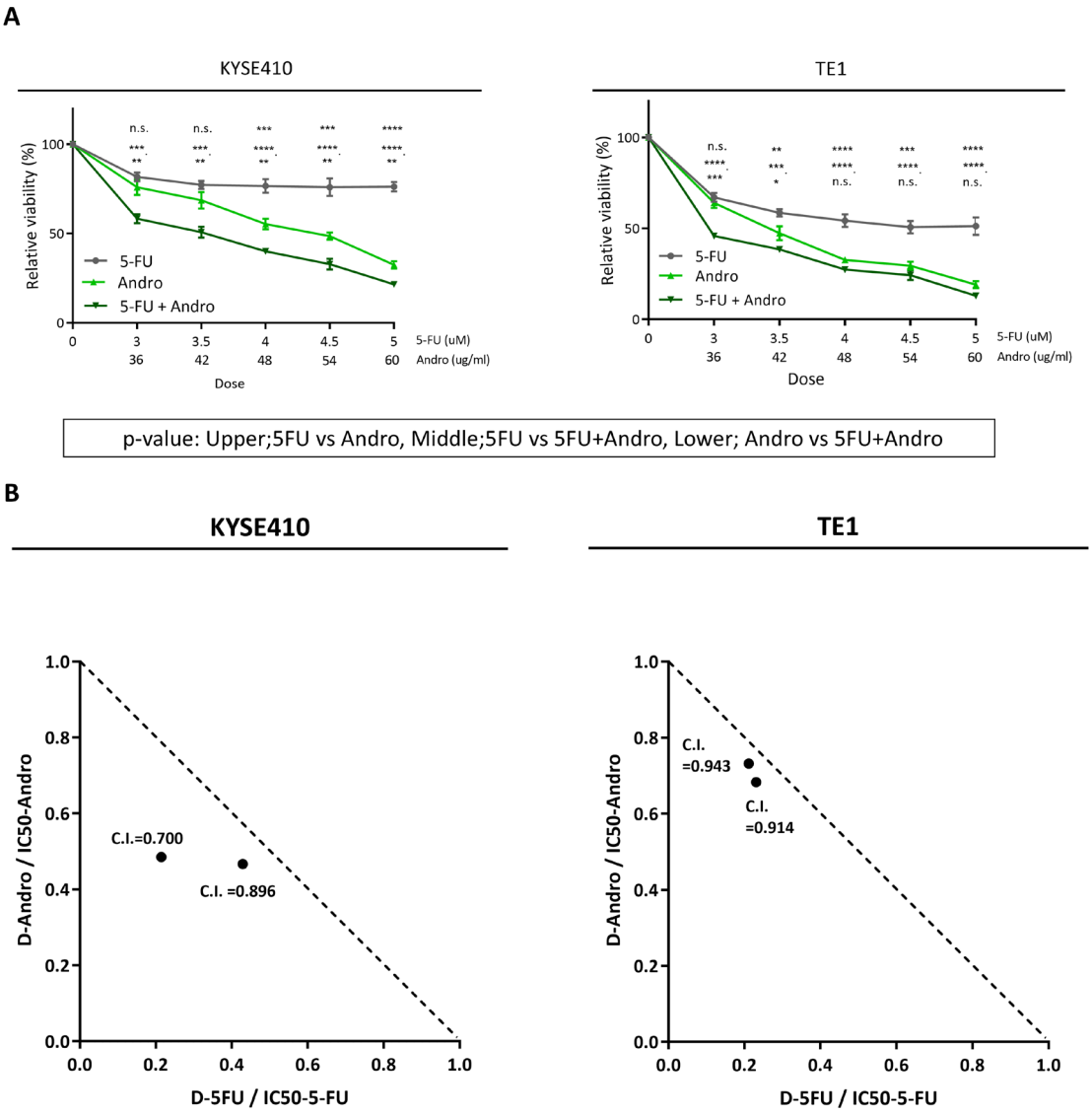

Figure 1. 5-FU and Andrographis inhibit the proliferation of esophageal squamous cell carcinoma cells. (A) WST assay was used to compare cell viability in KYSE410 and TE1 cells following treatment with 5-FU, Andrographis and the combination for 96 h. *P<0.05, **P<0.01, ***P<0.001 and ****P<0.0001 by one-way ANOVA followed by Tukey's post hoc test. (B) Isobologram including Chou-Talalay C.I. based on WST assay results to determine the additive effects of 5-FU and Andrographis in KYSE410 and TE1 cells. 5-FU, 5-fluorouracil; WST, Water Soluble Tetrazolium; C.I., combination index; n.s., not significant.

neutropenia, weight loss, and 5-FU-related gastrointestinal, hematologic, neurologic, and cardiovascular adverse events, which can limit dosing and worsen outcomes (31). These limitations highlight the need for adjunctive agents that can enhance 5-FU efficacy while reducing toxicity.

In the present study, Andrographis, a dietary compound with anti-inflammatory, antioxidant and immunomodulatory effects (8-13), was investigated as a potential therapeutic agent for ESCC. While its antitumor effects have been reported mainly in gastrointestinal adenocarcinomas (14-18), studies in SCC remain limited (22,23). The current *in vitro* experiments demonstrated that Andrographis significantly inhibited ESCC cell proliferation and colony formation and induced apoptosis, suggesting its efficacy extends to SCC. Notably, based on the patterns observed in the present data, TE1 and KYSE410 cells appear to differ in their responsiveness to cytotoxic stress. TE1 cells exhibited strong apoptotic responses to each single agent, suggesting that apoptosis pathways may be readily activated, which limits the remaining dynamic range for further enhancement by the combination treatment.

By contrast, KYSE410 cells demonstrated only modest apoptosis induction with both monotherapies, indicating a more refractory basal phenotype. Consequently, a wider dynamic range remains available, and the combination of 5-FU and Andrographis produced additive effect that was suggested to exceed the effect of 5-FU alone.

As one of the underlying mechanisms for its antitumor effect, focus was addressed on ferroptosis. Ferroptosis is a regulated cell death distinct from apoptosis and necrosis, characterized by lipid peroxide accumulation, mitochondrial dysfunction and hypoxia-inducible factor-1α activation (19-21). Dietary compounds have been shown to induce ferroptosis via diverse mechanisms. In colorectal adenocarcinoma, ginsenoside Rh3 suppresses SLC7A11 and activates Stat3/p53/NRF2 (32). Curcumin inhibits glutathione peroxidase 4 (GPX4) and SLC7A11 while modulating JNK and

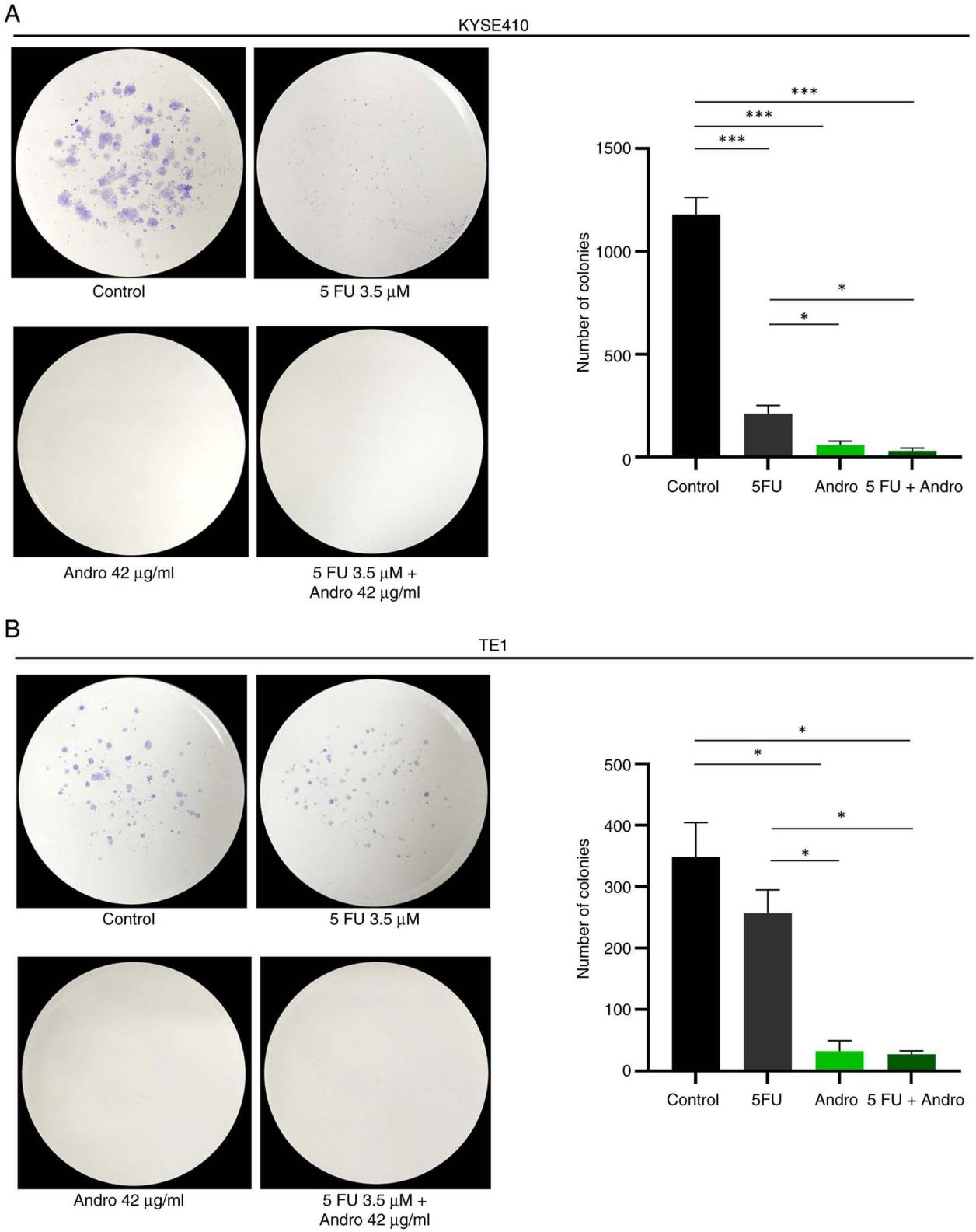

Figure 2. Inhibition of colony formation induced by 5-FU, Andrographis, and their combination in esophageal squamous cell carcinoma cells. (A and B) Colony formation assay was performed to evaluate the clonogenicity of (A) KYSE410 and (B) TE1 cells following treatment with 5-FU, Andrographis, and their combination. Images were calibrated using the known inner diameter (φ34.5 mm) of the 6-well plate. Optical magnification is not applicable. The white line at the bottom right represents a 10-mm scale bar. Bar graphs show the number of colonies in each treatment group. *P<0.05 and ***P<0.001 by one-way ANOVA with Tukey's post hoc test. 5-FU, 5-fluorouracil.

PI3K/Akt/mTOR (33,34) in gastric adenocarcinoma, arenobufagin upregulates Rev-erbα (35), and in ESCC, berbamine destabilizes GPX4 by downregulating USP51 (36). Based on previous studies, HMOX1, GCLC and GCLM were identified as the most consistently and reproducibly regulated ferroptosis-related genes in microarray analyses of gastrointestinal

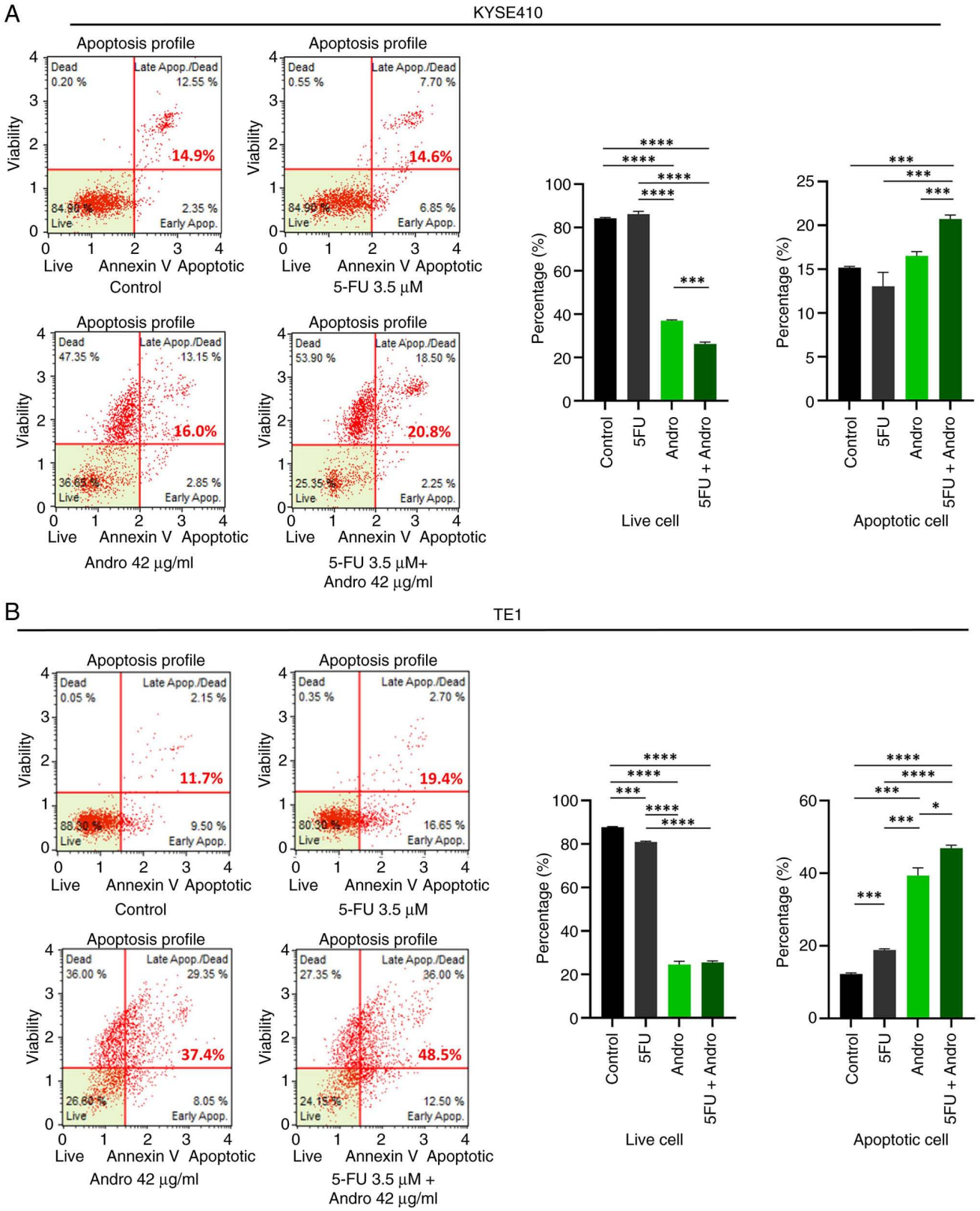

Figure 3. Combination of 5-FU and Andrographis enhances apoptotic activity in esophageal squamous cell carcinoma cells. (A and B) Representative images illustrating the percentage of cells undergoing apoptosis that stained positive for the Annexin-V assay in (A) KYSE410 and (B) TE1 cells. The assays were performed 72 h after treatment with each agent. The units were $\log_{10}$ transformed. Bar graphs show the percentage of live and apoptotic cells in each treatment group. *P<0.05, ***P<0.001 and ****P<0.0001 by one-way ANOVA followed by Tukey's post hoc test. 5-FU, 5-fluorouracil.

adenocarcinoma models treated with Andrographis (14-17). HMOX1 regulates iron metabolism and reactive oxygen species (ROS), thereby promoting ferroptosis (37-39), whereas GCLC and GCLM are essential for glutathione (GSH) synthesis and antioxidant defense via the antioxidant response element (ARE)-Nrf2 pathway (40-42). Because ferroptosis

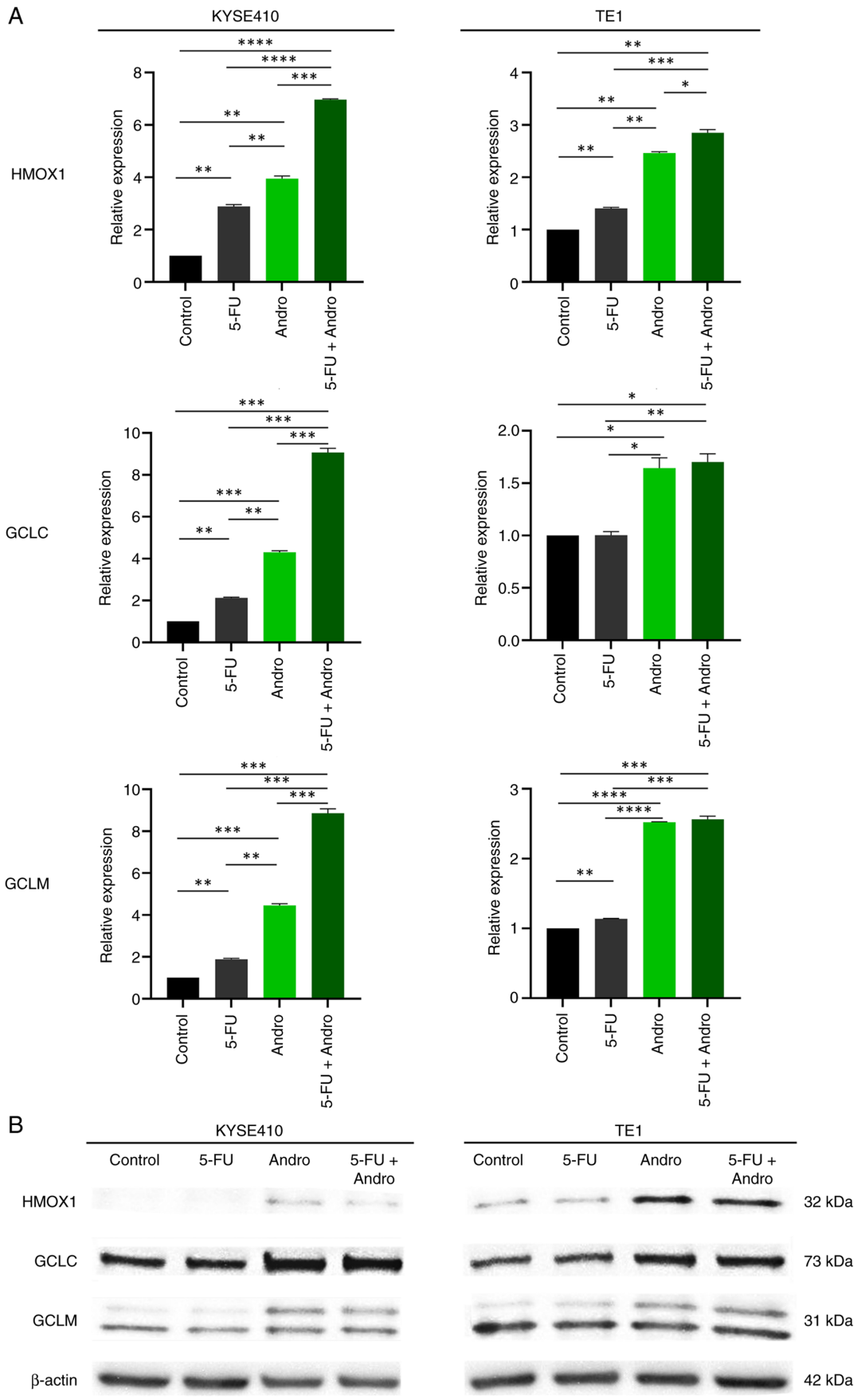

Figure 4. Altered mRNA and protein expression levels of the ferroptosis-associated targets HMOX1, GCLC and GCLM after 5-FU, Andrographis, and combination treatment in esophageal squamous cell carcinoma cells. (A) Changes in mRNA expression (HMOX1, GCLC and GCLM) after 5-FU, Andrographis and combination treatment in KYSE410 and TE1 cells. *P<0.05, **P<0.01, ***P<0.001 and ****P<0.0001 by one-way ANOVA with Tukey's post hoc test. (B) Representative images of western blotting assay of KYSE410 and TE1 cells treated as indicated. β-actin was used as the loading control. HMOX1, heme oxygenase-1; GCLC, glutamate-cysteine ligase catalytic; GCLM, glutamate-cysteine ligase modifier; 5-FU, 5-fluorouracil.

is driven by iron-dependent lipid peroxidation and disruption of cellular redox homeostasis, regulation of HMOX1 and glutathione synthesis pathways may reflect mechanistic processes linked to ferroptosis. In the present study, however, these transcriptional changes are interpreted as evidence of redox-related pathway modulation rather than definitive ferroptotic cell death, given the absence of direct lipid peroxidation or iron-dependent rescue assays. In the present study, redox-related pathways refer to cellular mechanisms that regulate oxidative stress, including iron metabolism and glutathione-dependent antioxidant systems. These observations suggest that such genes may have translational relevance as therapeutic targets not only in adenocarcinomas but also in SCCs. Therefore, HMOX1, GCLC and GCLM were selected as representative ferroptosis-associated genes in the present study. In KYSE410 cells, the combination markedly upregulated HMOX1, GCLC and GCLM, suggesting enhanced antioxidant responses that promote ferroptosis. By contrast, in TE1 cells, only HMOX1 was increased, whereas GCLC and GCLM changes were limited, indicating that the effect of 5-FU on GSH synthesis may depend on ESCC histological subtype. These molecular changes suggest that Andrographis may sensitize ESCC cells to alter redox homeostasis by inducing ferroptosis, consistent with previous findings in gastrointestinal adenocarcinoma cells. Regarding the alteration of mRNA-level for other ferroptosis regulators by RT-qPCR using cDNA derived from un-treated or post-treated ESCC cell-lines, GPX4 levels are downregulated after treatment by Andrographis in both ESCC cell-lines. GPX4 is a remarkable negative regulator of ferroptosis, which converts reduced GSH to oxidized glutathione and reduces lipid hydroperoxides, and it has been reported that GPX4 enhances ferroptosis in a MAPK/ERK kinase-, iron-, and ROS-dependent manner (43). Thus, in the present study, downregulation of GPX4 after Andrographis-treatment is expected hypothesis in consistency with the upregulation of HMOX1/GCLC/GCLM. On the other hand, upregulation of SLC7A11 after Andrographis-treatment was also shown in both ESCC cell-lines. SLC7A11 is a cystine/glutamate transporter, and SLC7A11-mediated cystine transportation plays an important role in suppressing ferroptosis by unchecked lipid peroxidation in cellular membranes (44), thus SLC7A11 is also known as a well-established negative regulator ferroptosis. It is suggested that the qPCR result of the present study for SLC7A11 which is opposite from hypothesis is induced because the ferroptosis-related pathway consists of not a simple but quite a complicated process including multiple genes (45), and positive- or negative-regulation of individual ferroptosis-related genes may occur by Andrographis-treatment. In future studies, further identification of down-stream ferroptosis-related target altered by Andrographis treatment is warranted.

Even at sub-IC50 doses of 5-FU, combining it with Andrographis enhanced antitumor effects, as shown by proliferation and apoptosis assays. Apoptosis and ferroptosis are not strictly independent modes of cell death; rather, they may potentially interact through several shared regulatory hubs associated with oxidative stress, such as intracellular iron homeostasis, mitochondrial ROS and lipid peroxidation (46,47). The ferroptosis-related gene alterations observed in the present study appear to be compatible with these previous observations and may indicate stress-response pathways that partially overlap with apoptosis. The current findings may provide preliminary insight into how these two pathways might interact.

Regarding clinical exposure, continuous infusion of 5-FU at 500-550 mg/m^2 over 24 h yielded a steady-state plasma concentration of ~120 ng/ml (0.923 μM) (48). While JCOG9907 and JCOG1109 did not report plasma concentrations of 5-FU (continuous infusion at 800 and 750 mg/m^2 over 24 h, respectively) (3), the current findings indicate that clinically achievable 5-FU levels are lower than the concentrations used in the present *in vitro* assays, where the IC_{50} values of 5-FU were 14.0 μM in KYSE410 cells and 4.5 μM in TE1 cells. The observed synergy suggests that combining Andrographis with 5-FU may allow for a reduction in the 5-FU dose while maintaining comparable cytotoxic effects.

The results of the present study indicate that Andrographis exerts antitumor effects by activating multiple cell death pathways, and its combination with 5-FU potentiates these effects. While the current *in vitro* findings require careful preclinical and clinical validation, they highlight Andrographis as a potential adjunctive strategy for ESCC treatment.

The present study has several limitations. First, a significant limitation is that the concentrations of 5-FU used in the *in vitro* experiments exceeded clinically achievable steady-state plasma levels (~0.9 μM), including the sub-IC_{50} doses. Thus, the observed synergy was obtained under supra-physiological conditions that may not fully reflect *in vivo* pharmacokinetics. The observed synergistic effects should not be interpreted as direct evidence for clinical application, but rather as preliminary mechanistic insights derived from *in vitro* experiments. Second, the clinical relevance of combining Andrographis with 5-FU requires rigorous *in vivo* validation under pharmacokinetically relevant conditions. Evaluation in appropriate animal or organoid models, together with assessment of toxicity and therapeutic window, will be essential to determine whether a clinically meaningful benefit can be achieved. These issues represent important objectives for future investigation. Third, it was confirmed that Andrographis treatment increased the expression of HMOX1, GCLC and GCLM; however, the detailed molecular mechanisms responsible for ferroptosis induction were not examined. Clarifying these mechanisms in future studies may help bridge basic research and clinical translation. Finally, the effects of Andrographis in 5-FU-resistant ESCC cells were not assessed in the present study. Because 5-FU resistance is multifactorial and often involves DNA damage-response alterations, determining whether Andrographis induces ferroptosis in resistant cells may provide insights for refining chemotherapy selection in ESCC.

In conclusion, the results of the present study indicate that Andrographis exerts antitumor effects on ESCC cells by inducing apoptosis and modulating ferroptosis-related transcriptional programs. When combined with low-dose 5-FU, these effects are additively enhanced, suggesting the potential of Andrographis as an adjunctive therapeutic strategy to improve efficacy while potentially reducing 5-FU dosage. Further studies are warranted to clarify the precise molecular mechanisms and to evaluate its efficacy in 5-FU-resistant ESCC models.

Acknowledgements

The authors would like to acknowledge Ms Amphone Okada and Ms Yuki Orito (Department of Gastrointestinal and Pediatric Surgery, Institute of Life Sciences, Mie University Graduate School of Medicine, Japan) for various technical suggestions, and Dr Gabrielle White Wolf (https://jp.edanz.com/ac) for editing a draft of this manuscript.

Funding

The present study was supported by Grants-in-Aid for Scientific Research (KAKENHI) (grant nos. 24K11846 and 25K11904).

Availability of data and materials

The data generated in the present study may be requested from the corresponding author.

Authors' contributions

KY, TS, YOku, RM, HY and YT conceived and designed the present study. KY and RM performed the experiments and analyzed the data. KY, TS and RM drafted the manuscript and prepared the figures. YH, TK, SY, YS, KH, MKa, YK, YOki, SY, MKo, MO, HO, ST and AG contributed to data acquisition and interpretation of the data. YOku and YT reviewed and revised the manuscript. All authors read and approved the final version of the manuscript. KY and TS confirm the authenticity of all the raw data.

Ethics approval and consent to participate

Not applicable.

Patient consent for publication

Not applicable.

Competing interests

The authors declare that they have no competing interests.

References

1. Bray F, Laversanne M, Sung H, Ferlay J, Siegel RL, Soerjomataram I and Jemal A: Global cancer statistics 2022: GLOBOCAN estimates of incidence and mortality worldwide for 36 cancers in 185 countries. CA Cancer J Clin 74: 229-263, 2024.
2. Lewis S and Lukovic J: Neoadjuvant therapy in esophageal cancer. Thorac Surg Clin 32: 447-456, 2022.
3. Ando N, Kato H, Igaki H, Shinoda M, Ozawa S, Shimizu H, Nakamura T, Yabusaki H, Aoyama N, Kurita A, *et al*: A randomized trial comparing postoperative adjuvant chemotherapy with cisplatin and 5-fluorouracil versus preoperative chemotherapy for localized advanced squamous cell carcinoma of the thoracic esophagus (JCOG9907). Ann Surg Oncol 19: 68-74, 2012.
4. Kato K, Machida R, Ito Y, Daiko H, Ozawa S, Ogata T, Hara H, Kojima T, Abe T, Bamba T, *et al*: Doublet chemotherapy, triplet chemotherapy, or doublet chemotherapy combined with radiotherapy as neoadjuvant treatment for locally advanced oesophageal cancer (JCOG1109 NExT): A randomised, controlled, open-label, phase 3 trial. Lancet 404: 55-66, 2024.
5. Hong P, Xu T, Xu J, Chen W, Hu H, Chen J, Li L, Zheng C, Li B, Liu J, *et al*: CD24 promotes metastasis and chemoresistance by directly targeting Arf6-ERK pathway in esophageal squamous cell carcinoma. Cancer Lett 594: 216994, 2024.
6. Yang X, Jiao Y, Zhang Y, Sun M, Gao Y, Zhou Y, Xiao H, Ren J, Zhou Z, Zhai Y, *et al*: Oseltamivir enhances 5-FU sensitivity in esophageal squamous carcinoma with high SPNS1. Biomed Pharmacother 173: 116367, 2024.
7. Li Z, Chen X, Li Y, Xu Y and Zhou Y: Aberrant DNA methylation in esophageal squamous cell carcinoma and its clinical implications in systemic chemotherapy. Int J Med Sci 22: 1002-1014, 2025.
8. Singh S, Pandey P, Ghosh S and Banerjee S: Anti-cancer labdane diterpenoids from adventitious roots of *Andrographis paniculata*: Augmentation of production prospect endowed with pathway gene expression. Protoplasma 255: 1387-1400, 2018.
9. Islam MT, Ali ES, Uddin SJ, Islam MA, Shaw S, Khan IN, Saravi SSS, Ahmad S, Rehman S, Gupta VK, *et al*: Andrographolide, a diterpene lactone from *Andrographis paniculata* and its therapeutic promises in cancer. Cancer Lett 420: 129-145, 2018.
10. Liu G and Chu H: Andrographolide inhibits proliferation and induces cell cycle arrest and apoptosis in human melanoma cells. Oncol Lett 15: 5301-5305, 2018.
11. Jayakumar T, Hsieh CY, Lee JJ and Sheu JR: Experimental and clinical pharmacology of *Andrographis paniculata* and its major bioactive phytoconstituent andrographolide. Evid Based Complement Alternat Med 2013: 846740, 2013.
12. Poolsup N, Suthisisang C, Prathanturarug S, Asawamekin A and Chanchareon U: *Andrographis paniculata* in the symptomatic treatment of uncomplicated upper respiratory tract infection: Systematic review of randomized controlled trials. J Clin Pharm Ther 29: 37-45, 2004.
13. Dai Y, Chen SR, Chai L, Zhao J, Wang Y and Wang Y: Overview of pharmacological activities of *Andrographis paniculata* and its major compound andrographolide. Crit Rev Food Sci Nutr 59 (Suppl 1): S17-S29, 2019.
14. Shimura T, Sharma P, Sharma GG, Banwait JK and Goel A: Enhanced anti-cancer activity of andrographis with oligomeric proanthocyanidins through activation of metabolic and ferroptosis pathways in colorectal cancer. Sci Rep 11: 7548, 2021.
15. Miyazaki K, Xu C, Shimada M and Goel A: Curcumin and andrographis exhibit Anti-tumor effects in colorectal cancer via activation of ferroptosis and dual suppression of glutathione Peroxidase-4 and ferroptosis suppressor Protein-1. Pharmaceuticals (Basel) 16: 383, 2023.
16. Ma R, Shimura T, Yin C, Okugawa Y, Kitajima T, Koike Y, Okita Y, Ohi M, Uchida K, Goel A, *et al*: Antitumor effects of andrographis via ferroptosis-associated genes in gastric cancer. Oncol Lett 22: 523, 2021.
17. Sharma P, Shimura T, Banwait JK and Goel A: Andrographis-mediated chemosensitization through activation of ferroptosis and suppression of beta-catenin/Wnt-signaling pathways in colorectal cancer. Carcinogenesis 41: 1385-1394, 2020.
18. Bao GQ, Shen BY, Pan CP, Zhang YJ, Shi MM and Peng CH: Andrographolide causes apoptosis via inactivation of STAT3 and Akt and potentiates antitumor activity of gemcitabine in pancreatic cancer. Toxicol Lett 222: 23-35, 2013.
19. Zhang Q, Deng T, Zhang H, Zuo D, Zhu Q, Bai M, Liu R, Ning T, Zhang L, Yu Z, *et al*: Adipocyte-Derived exosomal MTTP suppresses ferroptosis and promotes chemoresistance in colorectal cancer. Adv Sci (Weinh) 9: e2203357, 2022.
20. Li H, Yu K, Hu H, Zhang X, Zeng S, Li J, Dong X, Deng X, Zhang J and Zhang Y: METTL17 coordinates ferroptosis and tumorigenesis by regulating mitochondrial translation in colorectal cancer. Redox Biol 71: 103087, 2024.
21. Singhal R, Mitta SR, Das NK, Kerk SA, Sajjakulnukit P, Solanki S, Andren A, Kumar R, Olive KP, Banerjee R, *et al*: HIF-2α activation potentiates oxidative cell death in colorectal cancers by increasing cellular iron. J Clin Invest 131: e143691, 2021.
22. Yue GG, Lee JK, Li L, Chan KM, Wong EC, Chan JY, Fung KP, Lui VW, Chiu PW and Lau CB: *Andrographis paniculata* elicits anti-invasion activities by suppressing TM4SF3 gene expression and by anoikis-sensitization in esophageal cancer cells. Am J Cancer Res 5: 3570-3587, 2015.
23. Wang ZM, Kang YH, Yang X, Wang JF, Zhang Q, Yang BX, Zhao KL, Xu LP, Yang LP, Ma J, *et al*: Andrographolide radiosensitizes human esophageal cancer cell line ECA109 to radiation in vitro. Dis Esophagus 29: 54-61, 2016.

24. Stewart MJ and Watson ID: Standard units for expressing drug concentrations in biological fluids. Br J Clin Pharmacol 16: 3-7, 1983.
25. Takahashi M, Sung B, Shen Y, Hur K, Link A, Boland CR, Aggarwal BB and Goel A: Boswellic acid exerts antitumor effects in colorectal cancer cells by modulating expression of the let-7 and miR-200 microRNA family. Carcinogenesis 33: 2441-2449, 2012.
26. Schneider CA, Rasband WS and Eliceiri KW: NIH Image to ImageJ: 25 years of image analysis. Nat Methods 9: 671-675, 2012.
27. Livak KJ and Schmittgen TD: Analysis of relative gene expression data using real-time quantitative PCR and the 2(-Delta Delta C(T)) method. Methods 25: 402-408, 2001.
28. Chou TC: Drug combination studies and their synergy quantification using the Chou-Talalay method. Cancer Res 70: 440-446, 2010.
29. Jiaqi L, Siqing H, Qin W, di Z, Bei Z and Jialin Y: Andrographolide promoted ferroptosis to repress the development of non-small cell lung cancer through activation of the mitochondrial dysfunction. Phytomedicine 109: 154601, 2023.
30. Li W, Fu H, Fang L, Chai H, Ding B and Qian S: Andrographolide induced ferroptosis in multiple myeloma cells by regulating the P38/Nrf2/HO-1 pathway. Arch Biochem Biophys 742: 109622, 2023.
31. Katada C, Sugawara M, Hara H, Fujii H, Nakajima TE, Ando T, Kojima T, Watanabe A, Sakamoto Y, Ishikawa H, *et al*: A management of neutropenia using granulocyte colony stimulating factor support for chemotherapy consisted of docetaxel, cisplatin and 5-fluorouracil in patients with oesophageal squamous cell carcinoma. Jpn J Clin Oncol 51: 199-204, 2021.
32. Wu Y, Pi D, Zhou S, Yi Z, Dong Y, Wang W, Ye H, Chen Y, Zuo Q and Ouyang M: Ginsenoside Rh3 induces pyroptosis and ferroptosis through the Stat3/p53/NRF2 axis in colorectal cancer cells. Acta Biochim Biophys Sin (Shanghai) 55: 587-600, 2023.
33. Xin W and Zhang Y: Curcumin activates the JNK signaling pathway to promote ferroptosis in colon cancer cells. Chem Biol Drug Des 103: e14468, 2024.
34. Chen M, Tan AH and Li J: Curcumin represses colorectal cancer cell proliferation by triggering ferroptosis via PI3K/Akt/mTOR signaling. Nutr Cancer 75: 726-733, 2023.
35. Chen K, Li A, Wang J, Li D, Wang X, Liu C and Wang Z: Arenobufagin causes ferroptosis in human gastric cancer cells by increasing rev-erbalpha expression. J Tradit Complement Med 13: 72-80, 2023.
36. Peng H, He Y, Hu Y, Sheng S, Maitiyasen M, Li J, Liu Y, Hou X, Song H and Yi J: Berbamine promotes ferroptosis of esophageal squamous cell carcinoma by facilitating USP51-mediated GPX4 ubiquitination and degradation. Biomed Pharmacother 179: 117309, 2024.
37. Hassannia B, Wiernicki B, Ingold I, Qu F, Van Herck S, Tyurina YY, Bayır H, Abhari BA, Angeli JPF, Choi SM, *et al*: Nano-targeted induction of dual ferroptotic mechanisms eradicates high-risk neuroblastoma. J Clin Invest 128: 3341-3355, 2018.
38. Chen X, Yu C, Kang R and Tang D: Iron Metabolism in ferroptosis. Front Cell Dev Biol 8: 590226, 2020.
39. Tang D, Chen X, Kang R and Kroemer G: Ferroptosis: Molecular mechanisms and health implications. Cell Res 31: 107-125, 2021.
40. Lu CY, Yang YC, Li CC, Liu KL, Lii CK and Chen HW: Andrographolide inhibits TNFalpha-induced ICAM-1 expression via suppression of NADPH oxidase activation and induction of HO-1 and GCLM expression through the PI3K/Akt/Nrf2 and PI3K/Akt/AP-1 pathways in human endothelial cells. Biochem Pharmacol 91: 40-50, 2014.
41. Nishizawa H, Matsumoto M, Shindo T, Saigusa D, Kato H, Suzuki K, Sato M, Ishii Y, Shimokawa H and Igarashi K: Ferroptosis is controlled by the coordinated transcriptional regulation of glutathione and labile iron metabolism by the transcription factor BACH1. J Biol Chem 295: 69-82, 2020.
42. Huang CS, Lii CK, Lin AH, Yeh YW, Yao HT, Li CC, Wang TS and Chen HW: Protection by chrysin, apigenin, and luteolin against oxidative stress is mediated by the Nrf2-dependent up-regulation of heme oxygenase 1 and glutamate cysteine ligase in rat primary hepatocytes. Arch Toxicol 87: 167-178, 2013.
43. Yang WS, SriRamaratnam R, Welsch ME, Shimada K, Skouta R, Viswanathan VS, Cheah JH, Clemons PA, Shamji AF, Clish CB, *et al*: Regulation of ferroptotic cancer cell death by GPX4. Cell 156: 317-331, 2014.
44. Koppula P, Zhuang L and Gan B: Cystine transporter SLC7A11/xCT in cancer: Ferroptosis, nutrient dependency, and cancer therapy. Protein Cell 12: 599-620, 2021.
45. Zhou Q, Meng Y, Li D, Yao L, Le J, Liu Y, Sun Y, Zeng F, Chen X and Deng G: Ferroptosis in cancer: From molecular mechanisms to therapeutic strategies. Signal Transduct Target Ther 9: 55, 2024.
46. Endale HT, Tesfaye W and Mengstie TA: ROS induced lipid peroxidation and their role in ferroptosis. Front Cell Dev Biol 11: 1226044, 2023.
47. Neitemeier S, Jelinek A, Laino V, Hoffmann L, Eisenbach I, Eying R, Ganjam GK, Dolga AM, Oppermann S and Culmsee C: BID links ferroptosis to mitochondrial cell death pathways. Redox Biol 12: 558-570, 2017.
48. Kuwahara A, Yamamori M, Nishiguchi K, Okuno T, Chayahara N, Miki I, Tamura T, Kadoyama K, Inokuma T, Takemoto Y, *et al*: Effect of dose-escalation of 5-fluorouracil on circadian variability of its pharmacokinetics in Japanese patients with Stage III/IVa esophageal squamous cell carcinoma. Int J Med Sci 7: 48-54, 2010.